Performance Analysis of Sub-GHz System for IoT Applications

Kavitha Chandu, Ramesh Gorrepotu, Korivi Narendra Swaroop, and Madhavaprasad Dasari
Department of Electronics and Physics, GITAM Institute of Science, GITAM Deemed To Be University, Visakhapatnam – 530045, Andhra Pradesh, India
Email: kchandu@gitam.edu; {ramesh.gorrepotu; narendraswpk; madhavaprasaddasari}@gmail.com

***Abstract*—This article reports a sub-GHz, 868MHz, battery operated miniature sensor node with a fabricated helical Printed Circuit Board (PCB) and a third party whip antenna for Internet of Things (IoT) applications. CC1310 System on Chip (SoC), a sub-GHz family wireless microcontroller, is used to design the system. A HDC 1050 temperature and humidity sensor is interfaced with the microcontroller. The system has the desirable benefits of being small and inexpensive, long battery life and capable of long transmission range. The path loss exponent is calculated from Received Signal Strength Indicator (RSSI) values in two environments - free space and across concrete obstructions. A wireless sensor network is incorporated into a cloud platform for real time monitoring, and web application has been developed for data display and analysis. To validate the proposed IoT system, the measured data is compared with an independent meteorological data set from the Indian Meteorological Department, Cyclone Warning Centre, Visakhapatnam.**

***Index Terms*—CC1310 SoC, environmental monitoring, IoT, sub-GHz, 868MHz**

I. Introduction

Current and future Internet is expected to see spurts of data acquisition applications using Internet of Things (IoT) and cloud computing technologies [1]. These technologies extend the possibility of connecting remote devices [2]. The data acquired from things, such as sensors, is made available in a cloud environment [3]. Gubbi *et al*. presented a cloud centric vision for the IoT [4]. The integration of modern computing technologies such as data mining, machine learning and development of smart IoT systems is plausible in the near future [5]. For all the things in IoT, communication is the key factor. The paradigm of communication should enable seamless integration of things to the Internet. It develops new human being-to-device and device-to-device interactions [6]. Among the IoT application domains, the environmental monitoring receives a growing interest. Wireless Sensor Network (WSN) platforms are used for data acquisition in such indoor [7] and outdoor monitoring applications. Deployment of data acquisition systems is challenging in both scenarios, especially for open fields. Outdoor implementations may require large number of sensors, longer range, reduced power consumption and lower costs for design, deployment, operation and maintenance of the sensor nodes. At the same time, the nodes can be exposed to variable and extreme climatic conditions. A reusable WSN platform is suitable for use in low cost, long-term IoT environmental monitoring applications [8]. Various aspects of implementing sensor node networks have been studied. The data aggregation capacity of Wireless Sensor Networks has been reported to be dependent on the number of sensor nodes [9]. Secure interaction of sensor networks with the Internet is critical for protection of data against attacks. One of the implementations was using the base-station as a secure proxy for interfacing with network services [10]. Schemes for secure connectivity of WSNs with the Internet server are being developed with focus to reduce cost and energy consumption [11].

Wireless networks with minimal hardware and software like Bluetooth, Zigbee, GSM and Wi-Fi are useful to add things to Internet [12]-[15]. Use of GSM and Wi-Fi has shown less energy efficiency for IoT applications but are not able to cover large areas. Multihop wireless networks have been deployed with a suite of networking protocols with time delay constraints [16]. The key requirements in wireless networks are support for multiple nodes and large area coverage. For these requirements, the sensing devices must be small, energy efficient and cost-effective. In the sub-GHz spectrum, 868MHz has been used to address these requirements [17]-[22]. IoT sensor nodes using this spectrum can also handle interference better and enable the transmissions to weave between buildings in an urban environment. Transmission losses may become significant upon change in the environment of the nodes. Radio link quality estimation is known to have a fundamental impact on the network performance and it also affects the design of higher-layer protocols. The three factors that lead to link unreliability are the environment, interference and hardware transceivers. A set of four basic metrics, packet reception ratio, received signal strength indicator (RSSI), signal-to-noise ratio and link quality indicator, were considered in earlier works to characterize low-power links [23]. Due to wireless nature, the analysis of radio propagation plays an important role

Manuscript received June 11, 2020; revised August 20, 2020; accepted September 22, 2020.
Corresponding author: Madhavaprasad Dasari (email: madhavaprasaddasari@gmail.com)

doi: 10.18178/ijeetc.10.2.125-132

for performance evaluation. Path Loss Exponent (PLE) measured using RSSI has been considered by Miranda *et al*. for wireless communication analysis [24]. This article reports the design, benefits and propagation analysis of the IoT environmental monitoring system with a fabricated Printed Circuit Board (PCB) and a third party whip antenna operating at 868MHz. For the transmission range analysis, two environments – free space and in-building were chosen. The PLE is calculated from measured RSSI values.

The remaining sections of this paper are organized as follows. Section II deals with hardware, software, web interface, antenna and other desirable features of the deployed system. Section III deals with the analysis of transmission range. Section IV compares the acquired sensor data from our system with an independent set from Indian Meteorological Department (IMD), Government of India.

II. Analysed Sub-GHz IoT System

Our deployed system consists of sub-GHz board (SoG), a sensor node and a gateway. The sub-GHz board is developed using CC1310 SoC (system on chip), a sub-GHz family wireless microcontroller. The sensor node is a combination of sub-GHz board and a small sensor board to interface sensors. For our present study temperature and humidity sensors were considered. The gateway is a combination of sub-GHz board and Raspberry Pi 3 (RPi3).

A typical wireless gateway-sensor network deployment scenario is shown in Fig. 1. Our wireless gateway-sensor network is deployed with two sensor nodes and each is interfaced with digital sensors for temperature and humidity measurement. In order to reduce the power consumption, the sensor board collects the sensed data every minute and returns to sleep mode. The nodes broadcast collected data through Radio Frequency (RF) interface to gateway using 868MHz. The gateway receives data from the nodes locally and uploads them to the cloud. The stored data in cloud can be accessed using a web application. Data from a particular node can be obtained by selecting the sensor Id. Ajax java script is used to display the web pages. A detailed description of the used hardware and implemented software can be found in [25].

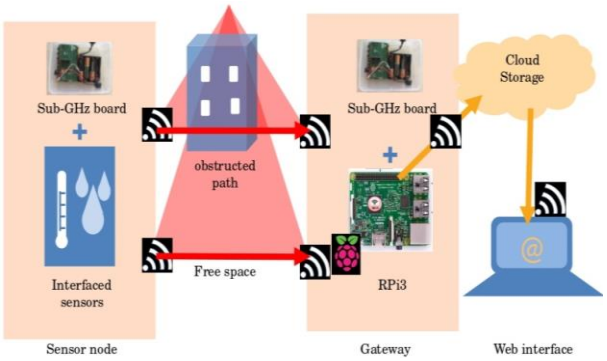

Fig. 1. Generic architecture of sub-GHz system

In Fig. 1, Sensors (like humidity and temperature) are interfaced with the sub-GHz board. This forms the sensor node. Data transmission takes place at 868 MHz across free space or concrete obstructions. This data is received at the gateway (A RPi3 and a sub-GHz board) and pushed to the cloud. A web interface is used to access the stored data.

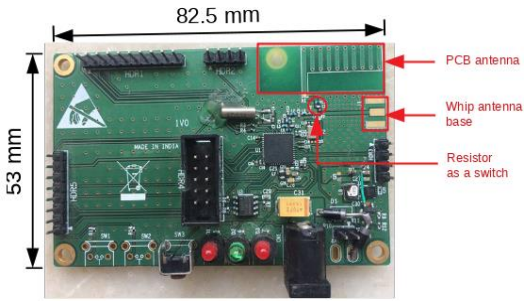

Fig. 2. Sub-GHz board with CC1310 SoC.

A. Hardware

1) CC1310 sub-GHz board

CC1310 SoC is a single chip solution incorporating a complete RF system and an on-chip direct current (DC-DC) converter. Our sub-GHz board (Fig. 2) was designed using CC1310 SoC which has two different advanced RISC machines (ARM) cores on a single chip. One is Cortex®-M3 for peripheral control and supplies internal power to the RF core. The other core is an ARM Cortex®-M0 which is dedicated for the RF functionality. The CC1310 SoC combines a flexible low power RF transceiver and a powerful 48 MHz Cortex®-M3 microcontroller. This is done on a platform supporting multiple physical layers and RF standards. The low level RF protocol commands are stored in ROM/RAM, and handled by a radio controller Cortex®-M0. This ensures ultra-low power and flexibility. The low-power consumption of the CC1310 SoC device does not come at the expense of RF performance. Excellent sensitivity and robustness is shown by CC1310. The RF section comes with a programmable output power up to +14dBm. The receiver sensitivity is −124dBm in long-range mode, −110dBm at 50kbps, selectivity is 52dB and blocking performance 90 dB. It has a single-ended or differential RF physical interface. The advantage of this RF core is a wireless M-bus and IEEE 802.15.4g PHY interface that receives and transmits the RF data packets. A (G) Frequency Shift Keying (FSK) modulation technique is used to transmit and receive the RF packets from the CC1310 RF core. The sub-GHz with −95dBm sensitivity is suitable for environmental monitoring applications [26].

2) Sensor node

The sub-GHz board can interface with external devices using built-in interfaces. The corresponding signal pins are extended to a 10-pin header for the interface to small sensor board (Fig. 3). The serial peripheral interface (SPI) interface signals are extended to 6-pin header connected to external flash of various sizes for the local storage. For observing relative humidity and temperature, a Texas Instruments (TI) based HDC 1050/HDC 1080 is considered. The sub-GHz board at the node acts as a sensor data carrier via sub-GHz wireless communication.

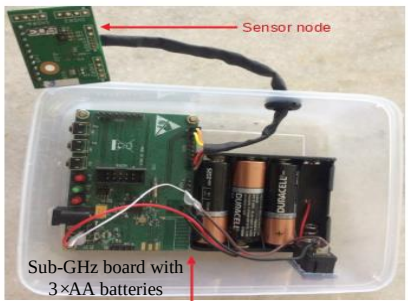

Fig. 3. Sensor node: Sub-GHz board with sensor.

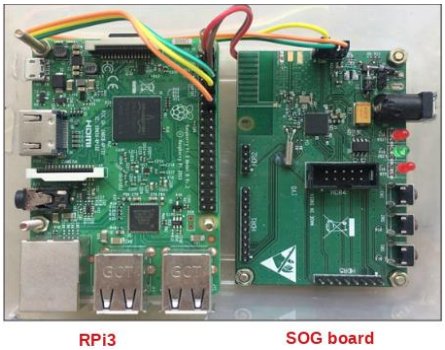

Fig. 4. Gateway: Sub-GHz board with RPi3.

3) Gateway

The Gateway node is a combination of sub-GHz board and RPi3 (Fig. 4). The gateway receives sensed data through 868MHZ sub-1GHz RF interface, and sends the received data to raspberry Pi through universal asynchronous receiver/transmitter (UART) interface with a baud rate 115200bps. RPi3 processes the data at Gateway and pushes the data to cloud through message queuing telemetry transport (MQTT) protocol over TCP/IP. Light emitting diodes (LEDs) are used in the gateway node to represent the reception and transmission status of RF packets. The Gateway has 128KB of ROM and 8KB of RAM for system operation. The device can transmit or receive maximum of 500 Kilobytes. The maximum data rate limit of the microcontroller chip is 4000kbps. The RPi3 uses a secure digital (SD) card memory for its operation. 1G RAM is used to process the code. The sub-GHz board at the gateway acts as an RF receiver for 868MHz and transfers the data to RPi3 using serial communication.

B. Software Description

The present system uses open source software and operating system in addition to some in-house code for the firmware. The interfaces were coded using readily available tools and standard protocols. Specifically, the following tools have been used for software development

i) Sub-GHz board firmware: Embedded C with TI RTOS
ii) Operating system: Raspibian
iii) IoT web application and tools
- UI: HTML5, CSS3 Backend: PHP
- Database: ORACLE
- Services: REST-API (JSON)
- Server: Apache http 2.2

iv) Messaging protocol: MQTT

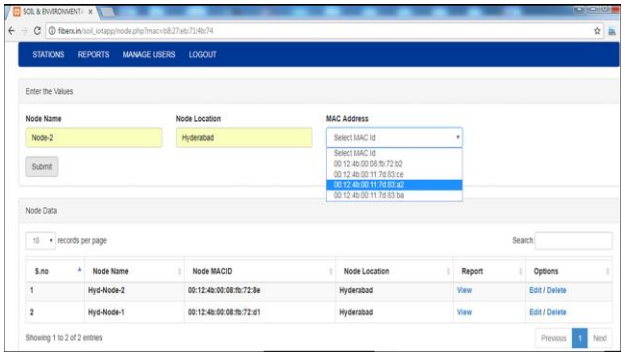

Fig. 5. A snapshot of the designed web interface.

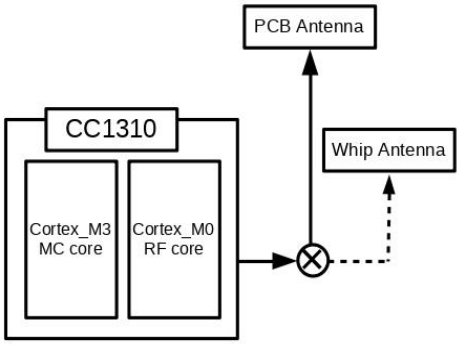

Fig. 6. Block diagram of the RF interface. The CC1310 SoC can be interfaced with the fabricated helical PCB or the third party whip antenna at a time.

C. Web Interface

For data accessibility in real-time from anywhere, the wire-less sensor network is incorporated into cloud platform. A web application is developed for data display from different nodes located in different places. Different IDs are set for each sensor node. Data from a particular node can be obtained by selecting the sensor ID (Fig. 5).

The web application is designed using PHP and HTML languages. Ajax java script is used for data request from the database and to display the web pages. Oracle database is used for the storage of sensors' data, which are received from the sensor nodes.

D. Antenna

The present system is tested at 868MHz with fabricated helical PCB antenna and third party whip antenna at gateway and sensor node. Our measurements were performed with the whip and PCB antenna oriented vertically and horizontally, respectively. The CC1310 SoC can be interfaced with either of the antennae using resistor as a switch (Fig. 6).

1) Fabricated helical PCB antenna

A helical PCB antenna (Fig. 7) is fabricated for sub-GHz frequency as a 2-layer PCB. During the fabrication the important parameter considered is distance between ground plane and antenna. The fabricated PCB-antenna was tested with Agilent Technologies, E5071C ENA series network analyzer for center frequency and voltage standing wave ratio (VSWR, a numerical parameter which gives antenna impedance matching to radio/ transmission line it is connected). An impedance matching of 50 ohms is achieved. VSWR less than 3.8 is a measure of its good transmission at 868MHz [8].

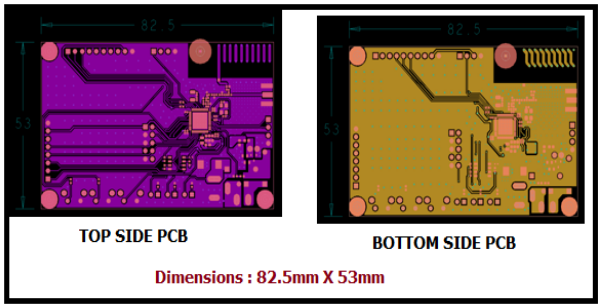

Fig. 7. The layout of the sub-GHz board along with PCB antenna. See Fig. 2 for the antenna.

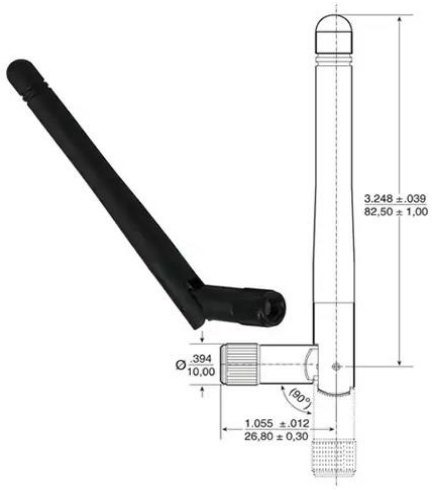

Fig. 8. Dimensions of the third party whip antenna.

2) Whip antenna

A third party whip antenna (Fig. 8) was tested for centre frequency and VSWR. The VSWR for PCB antenna is 3.6558 at 868MHz and for whip antenna is 1.3715 at the same frequency.

E. Features

This system, like other IoT systems, is scalable in terms of number of deployed transmitter and receiver nodes. As a result, reduced size, cost and consumed power are desirable features.

1) Size of sensor node

The SoG board with small physical size is designed. The node size is 53mm ×82.5mm.

2) Cost of the unit

As sub-GHz is opted for IoT applications; the present node is developed with low cost. The cost of the SoG board is approximately $17.49 (Table I). The cost is relatively low when compared to similar IoT applications.

TABLE I: COST OF THE SOG BOARD

Item	Price (US $)
CC1310 Chip	3.10
LDO	1.99
Crystals	1.30
Active and Passive Components	4.00
Power Adapter	1.30
Outer casing	3.00
PCB	2.80
PCB Antenna	0.00
Total cost	**17.49**

3) Predicted battery life

The designed sensor node is tested for its power consumption as it is a critical issue for battery-powered wireless sensor nodes. The sensor node in the present system is powered through 3×AA batteries with a capacity of 1500mAh. Battery life is computed as follows

$$Battery\ life = \frac{\text{Battery capacity mAh}}{\text{Load capacity mA}} \quad (1)$$

TABLE II: BATTERY LIFE ANALYSIS

Sensor type (Digital)	Load current consumption (mA)	Battery life (Days)
Mode 1	0.01	6250
Mode 2	0.02	3125

The power consumption for two different operation modes is tabulated in Table II.

Mode 1: Current is measured at sensor node when the system is in idle state. Idle state is defined as that when sensor node is powered ON and with no sensor activated.

Mode 2: In this mode, the current consumption is calculated when the sensor is sampling once every minute along with RF transmission.

The designed node with no sensor activated, the 1500mAh batteries can last up to 6250 days. With temperature and humidity sensor operating along with RF transmission, the batteries should sustain up to 3125 days.

III. TRANSMISSION RANGE ANALYSIS

RSSI parameterizes the signal strength and the failure of communication between transmitter and receiver by their separation. RSSI values were measured using the PCB and whip antenna. In free space (measured up to 250m) the RSSI ranged from –38 dB to –88dB and across concrete obstructions (measured up to 20m) from –32 dB to –94dB. The Path Loss Exponent (PLE) in radio signal propagation is considered for assessment of power loss in signal transmission from sensor node to gateway. The RSSI values recorded are used to calculate the path loss exponent. In general, path loss may occur due to many surrounding factors such as reflection, fading, diffraction, shadowing, etc. In all distance dependent models, the path loss exponent is an important parameter and is given by

$$\text{Path loss} = PL(d_0) + 10n\log10(d/d_o) \quad (2)$$

where $PL(d_0)$ is path loss with respect to a given reference distance d_0, d the transmitter-receiver separation and n is the path loss exponent.

With different combinations of antenna at node and gateway, the RSSI values obtained from 1m to 250m and an average of 25 samples were taken at each value of d. All possible combinations of the fabricated PCB and third party whip antenna were considered at the transmitter and receiver nodes to validate an acceptable performance of the PCB antenna. It is clear from (2) that the slope of the linear fit is the value of n. The PLE values measured using RSSI are compared with theoretical values given in literature. For free space the value is known to be 2 and for concrete obstructions it is known to be between 4 and 6 [27]. For path loss assessment, the field trials were conducted at GITAM (deemed to be University), Visakhapatnam, Andhra Pradesh.

A. *Free Space*

Fig. 9. (Top) Map of the field trial location. (Bottom) The red circles mark the locations of receiving third party whip antenna (lower left) and transmitting PCB antenna (upper right). The transmission takes place in free space along the line of sight marked by the red line in the map.

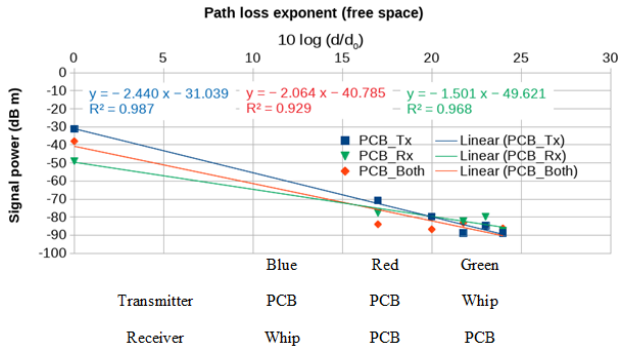

Fig. 10. Free space transmission: Average RSSI values for the tabulated combinations of antennas at the receiver and transmitter nodes. Linear fits to Equation 2 are used to estimate the PLE.

Observations were taken with the gateway fixed at a location in free space and the sensor node was moved to change their relative separation. The test was repeated for several distances along line of sight (LoS) from 1m to 250m. For the longest distance tested, the gateway was placed above a thirteen storeyed building in free space and the sensor node was placed on nine storeyed building 1.2 kilometer away from gateway. The measurement locations are shown in the Fig. 9 (top) with the line of sight (LoS) in red. The case of whip antenna at the gateway and PCB at sensor node for the longest distance tested is shown in Fig. 9 (bottom).The received RSSI values at different instances indicated at gateway are plotted in Fig. 10 with whip and PCB antenna combinations. The obtained PLE value for the first combination of antennas in Table III is 2.439 in free space. This was obtained by fitting Equation 2 to the averaged out data set of 25 samples per separation (blue curve in Fig. 10). The second and third combinations of antennas in Table III yield the values of 2.064 and 1.50, respectively (red and green curves of Fig. 10). The measurements were performed in a stadium with the gateway placed in the gallery which is about 25 feet above the ground level. The sensor node was positioned along the ground. The radiation pattern of the helical PCB antenna is known to be anisotropic. In this case a change in the relative orientations of antennae affected the PLE values significantly.

TABLE III: PLE ASSESSMENT – FREE SPACE

TX:NODE (Transmitter)	RX: Gateway (Receiver)	PLE
PCB	Whip	2.439
PCB	PCB	2.064
Whip	PCB	1.5

Fig. 11. Gateway placed inside a room for reception across concrete obstructions.

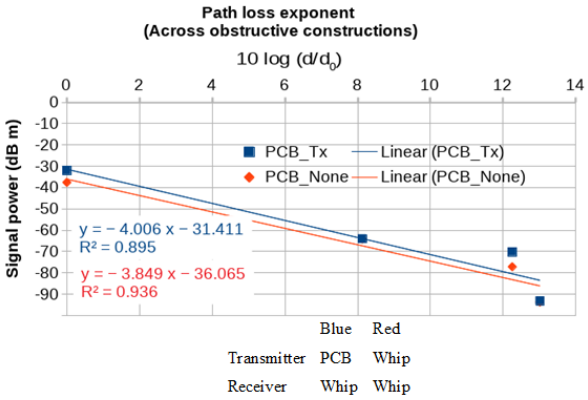

Fig. 12. Transmission across obstructive constructions: Average RSSI values for the tabulated combinations of antennas at the receiver and transmitter nodes. Linear fits to Equation 2 are used to estimate the PLE.

B. *Across Concrete Obstructions*

Concrete is widely known to cause significant wireless signal attenuation depending on the formulation, thickness of the concrete and iron or steel reinforcements. Path loss will occur from many sources within the building – separation, distance, reflection, diffraction, absorption, shadowing and multipath reception. For this scenario the gateway was placed inside a concrete room (Fig. 11). The node is placed in different rooms, in the same floor of the building, separated with wall thickness of 27cm and distance measured is up to 20m. The values obtained are plotted as shown in Fig. 12.

TABLE IV: PLE ASSESSMENT – ACROSS CONCRETE OBSTRUCTIONS IN A BUILDING

TX:NODE (Transmitter)	RX: Gateway (Receiver)	PLE
PCB	Whip	4.006
Whip	Whip	3.849

From Table IV it is clear that the designed system works in an environment with obstructive constructions and may be deployed in industrial, scientific and medical setups.

IV. SENSOR DATA VALIDATION

A web application has been developed for data recording and analysis. The application can be browsed at http://fiberx. in/soil_iotapp/index.html. Data is fetched from the web server and displayed on the home screen. The most recent readings of the sensor parameters are displayed on the web page from a selected sensor node. To validate the measured temperature and humidity data, it is compared with the meteorological data recorded by India Meteorological Department, Cyclone Warning Centre, Government of Visakhapatnam, India. It is known that their measurements are taken according to the World Meteorological Organization standards. The typical values of accuracy for HDC1050 are ±3% for relative humidity and ±0.2°C for temperature. Our data was collected with the sensor node placed inside a room. The difference in temperature measurement from the two sources is not more than 5.04%. For humidity measurements, the difference was up to 5.56%. The errors beyond the accuracy of the sensors would be due to the local variations of the measured parameters at the sensor node location. The obtained results for temperature and humidity are tabulated for comparison in Table V and Table VI and plotted in Fig. 13 respectively.

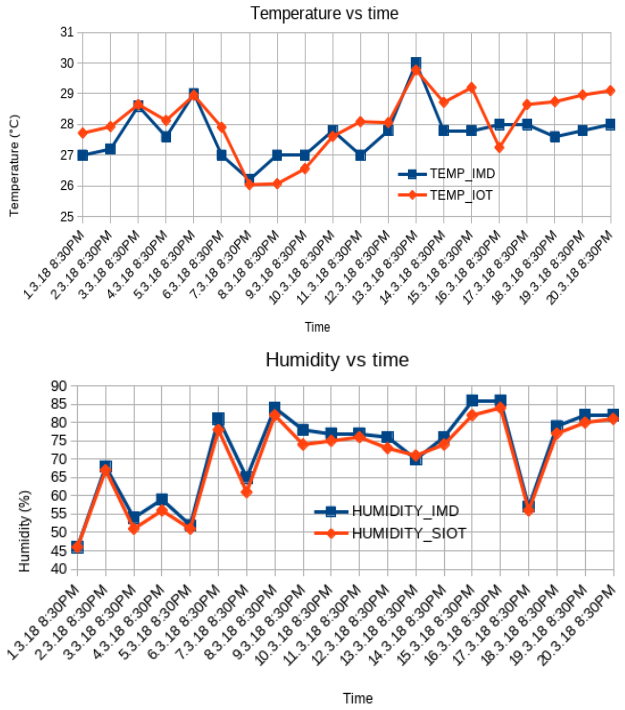

Fig. 13. Comparison of the temperature (top) and humidity (bottom) data acquired from our IoT system with that of IMD, CWC, Visakhapatnam, India.

TABLE V: COMPARISON OF TEMPERATURE FROM IOT SYSTEM AND IMD, VISAKHAPATNAM, INDIA

DATE & TIME	TEMP IMD	TEMP IoT	Error (%)
1.3.18 8:30PM	27	27.72	0.03
2.3.18 8:30PM	27.2	27.93	2.68
3.3.18 8:30PM	28.6	28.65	0.17
4.3.18 8:30PM	27.6	28.13	1.92
5.3.18 8:30PM	29	28.95	0.17
6.3.18 8:30PM	27	27.91	3.37
7.3.18 8:30PM	26.2	26.04	0.61
8.3.18 8:30PM	27	26.07	3.44
9.3.18 8:30PM	27	26.56	1.63
10.3.18 8:30PM	27.8	27.61	0.68
11.3.18 8:30PM	27	28.09	4.04
12.3.18 8:30PM	27.8	28.06	0.94
13.3.18 8:30PM	30	29.77	0.77
14.3.18 8:30PM	27.8	28.72	3.31
15.3.18 8:30PM	27.8	29.2	5.04
16.3.18 8:30PM	28	27.25	2.68
17.3.18 8:30PM	28	28.65	2.32
18.3.18 8:30PM	27.6	28.74	4.13
19.3.18 8:30PM	27.8	28.96	4.17
20.3.18 8:30PM	28	29.1	3.93
Mean	**27.71**	**28.1055**	

Note: The *p*-value is 0.186538. The result is not significant at $p<0.05$

TABLE VI: COMPARISON OF HUMIDITY FROM IOT SYSTEM AND IMD, VISAKHAPATNAM, INDIA

Date & time	Humidity IMD	Humidity IoT	Error (%)
1.3.18 8:30PM	46	46	0
2.3.18 8:30PM	68	67	1.47
3.3.18 8:30PM	54	51	5.56
4.3.18 8:30PM	59	56	5.08
5.3.18 8:30PM	52	51	1.92
6.3.18 8:30PM	81	78	3.7
7.3.18 8:30PM	65	61	6.15
8.3.18 8:30PM	84	82	2.38
9.3.18 8:30PM	78	74	5.13
10.3.18 8:30PM	77	75	2.6
11.3.18 8:30PM	77	76	1.30
12.3.18 8:30PM	76	73	3.95
13.3.18 8:30PM	70	71	1.43
14.3.18 8:30PM	76	74	2.63
15.3.18 8:30PM	86	82	4.65
16.3.18 8:30PM	86	84	2.33
17.3.18 8:30PM	57	56	1.75
18.3.18 8:30PM	79	77	2.53
19.3.18 8:30PM	82	80	2.44
20.3.18 8:30PM	82	81	1.22
Mean	**71.75**	**69.75**	

Note: The *p*-value is 0.603637. The result is not significant at $p<0.05$

The data obtained from the designed system and recorded meteorological data by India Meteorological Department, are subject to statistical analysis. Anova test is applied and results show that the difference between two measurements is not statistically significant rejecting the hypothesis that they are significantly different.

V. CONCLUSION

In conclusion, we have successfully validated an IoT system at 868MHz with combinations of a fabricated low-cost helical PCB antenna and a third party whip antenna with cloud access. Our system is power efficient running on 3×AA batteries for about 3125 days and can be used for communications up to 1.2 km in free space and at least 20m in buildings across obstructive concrete walls. The PCB antenna with its small size can be used effectively in applications with size constraints as in medical fields. Other applications with relaxed size

constraints, a whip antenna can find a use. This should serve as a prototype for IoT applications in the unlicensed and rather less used frequency of 868MHz.

CONFLICT OF INTEREST

The authors declare no conflict of interest.

AUTHOR CONTRIBUTIONS

Kavitha chandu, Ramesh Gorrepotu and Korivi Narendra Swaroop conducted the research. Design, fabrication, software development and implementation part was carried out by the above said authors. Madhava parsad Dasari analysed the data and the paper was written by Kavitha chandu. All authors had approved the final version.

ACKNOWLEDGMENT

The authors acknowledge the Indian Meteorological Department, Cyclone Warning Centre, Government of India, Visakhapatnam for providing the temperature and humidity data.

REFERENCES

[1] A. Botta, W. De Donato, V. Persico, and A. Pescapé, "Integration of cloud computing and internet of things: A survey," *Future Generation Computer Systems*, vol. 56, pp. 684–700, Mar. 2016.

[2] S. Chen, H. Xu, D. Liu, B. Hu, and H. Wang, "A vision of IoT: Applications, challenges, and opportunities with china perspective," *IEEE Internet of Things Journal*, vol. 1, no. 4, pp. 349–359, 2014.

[3] B. Kantarci and H. T. Mouftah, "Trustworthy sensing for public safety in cloud-centric internet of things," *IEEE Internet of Things Journal*, vol. 1, no. 4, pp. 360–368, 2014.

[4] J. Gubbi, R. Buyya, S. Marusic, and M. Palaniswami, "Internet of things (IOT): A vision, architectural elements, and future directions," *Future Generation Computer Systems*, vol. 29, no. 7, pp. 1645–1660, 2013.

[5] C. W. Tsai, C. F. Lai, and A. V. Vasilakos, "Future internet of things: Open issues and challenges," *Wireless Networks*, vol. 20, no. 8, pp. 2201–2217, 2014.

[6] C. Anton-Haro and M. Dohler, *Machine-to-Machine (M2M) Communications: Architecture, Performance and Applications*, Elsevier, 2014.

[7] B. Bellekens, R. Penne, and M. Weyn, "Realistic Indoor Radio Propagation for Sub-GHz Communication," *Sensors (Basel)*, vol. 18, no. 6, Jun. 2018.

[8] M. T. Lazarescu, "Design of a WSN platform for long-term environmental monitoring for IoT applications," *IEEE Journal on Emerging and Selected Topics in Circuits and Systems*, vol. 3, no. 1, pp. 45–54, 2013.

[9] C. Wang, C. Jiang, Y. Liu, X. Y. Li, and S. Tang, "Aggregation capacity of wireless sensor networks: Extended network case," *IEEE Trans. on Computers*, vol. 63, no. 6, pp. 1351–1364, 2014.

[10] R. Roman and J. Lopez, "Integrating wireless sensor networks and the internet: A security analysis," *Internet Research*, vol. 19, no. 2, pp. 246–259, 2009.

[11] M. E. S. Saeed, Q. Liu, G. Tian, B. Gao, and F. Li, "HOOSC: Heterogeneous online/offline signcryption for the internet of things," *Wireless Networks*, vol. 24, pp. 3141–3160, May 2017.

[12] A. A. Sabbagh, P. Pupatwibul, A. Banjar, and R. Braun, "Optimization of the open flow controller in wireless environments for enhancing mobility," in *Proc. 38th Annual IEEE Conf. on Local Computer Networks*, 2013, pp. 930–935.

[13] A. Lambebo and S. Haghani, "A wireless sensor network for environmental monitoring of greenhouse gases," presented at the ASEE 2014 Zone I Conf. University of Bridgeport, Bridgpeort, CT, 2014.

[14] C. M. Nguyen, J. Mays, D. Plesa, S. Rao, M. Nguyen, and J. C. Chiao, "Wireless sensor nodes for environmental monitoring in internet of things," in *Proc. IEEE MTT-S Int. Microwave Symposium*, 2015, pp. 1–4.

[15] M. S. Jamil, M. A. Jamil, A. Mazhar, A. Ikram, A. Ahmed, and U. Munawar, "Smart environment monitoring system by employing wireless sensor networks on vehicles for pollution free smart cities," *Procedia Engineering*, vol. 107, pp. 480–484, 2015.

[16] J. Yang and X. Li, "Design and implementation of low-power wireless sensor networks for environmental monitoring," in *Proc. IEEE Int. Conf. on Wireless Communications, Networking and Information Security*, 2010, pp. 593–597.

[17] G. Bragg, K. Martinez, P. Basford, and J. Hart, "868mhz 6lowpan with contikiMAC for an internet of things environmental sensor network," in *Proc. SAI Computing Conf.*, 2016, pp. 1273–1277.

[18] J. Muñoz, T. Chang, X. Vilajosana, *et al*., "Evaluation of IEEE802.15.4g for environmental observations," *Sensors (Basel)*, vol. 18, no. 10, Oct. 2018.

[19] B. Bellekens, R. Penne, and M. Weyn, "Realistic indoor radio propagation for sub-GHz communication," *Sensors (Basel)*, vol. 18, no. 6, Jun. 2018.

[20] Y. Yin, L. Xiong, Y. Zhu, B. Chen, H. Min and H. Xu, "A compact dual-band digital doherty power amplifier using parallel-combining transformer for cellular NB-IoT applications," in *Proc. IEEE International Solid-State Circuits Conference*, San Francisco, CA, 2018, pp. 408-410.

[21] E. De Poorter, J. Hoebeke, M. Strobbe, *et al*., "Sub-GHz LPWAN network coexistence, management and virtualization: An overview and open research challenges," *Wireless Pers. Commun*, vol. 95, pp. 187–213, Jun. 2017.

[22] J. Famaey, R. Berkvens, G. Ergeerts, *et al*., "Flexible multimodal sub-gigahertz communication for heterogeneous internet of things applications," *IEEE Communications Magazine*, vol. 56, no. 7, pp. 146-153, July 2018.

[23] N. Baccour, A. Koubâa, L. Mottola, M. A. Zúñiga, H. Youssef, C. A.Boano, and M. Alves, "Radio link quality estimation in wireless sensor networks: A survey," *ACM Trans. on Sensor Netw.*, vol. 8, no. 4, pp. 34-38, 2012.

[24] J. Miranda, R. Abrishambaf, T. Gomes, P. Gonçalves, J. Cabral, A. Tavares, and J. Monteiro, "Path loss exponent analysis in wirelesssensor networks: Experimental evaluation," in *Proc. 11th IEEE Int. Conf. on Industrial Informatics*,. 2013, pp. 54–58.

[25] R. Gorrepotu, N. S. Korivi, K. Chandu, and S. Deb, "Sub-1GHz miniature wireless sensor node for IoT applications," *Internet of Things*, vol. 1-2, pp. 27–39, Sep. 2018.

[26] A. Silva, "Duty-cycled, sub-GHz wake-up radio with -95dBm sensitivity and addressing capability for environmental monitoring applications," presented at IEEE 10th Annual Ubiquitous Computing, Electronics & Mobile Communication Conference, New York, 2019.

[27] L. Atzori, A. Iera, and G. Morabito, "The internet of things: A survey," *Computer Networks*, vol. 54, no. 15, pp. 2787–2805, 2010.

Dr. Kavitha Chandu is Associate Professor in the Department of Electronics/ Physics, GITAM Institute of Science, GITAM (deemed to be) University, Visakhapatnam. She has about 24 years of service in the academia. She obtained M.Sc (tech), M.Phil and Ph.D. from Andhra University, Visakhapatnam. She also received M.Tech (CSE) from Acharya Nagarjuna University, Guntur. She has published extensively in the areas of Embedded Systems, Digital Signal Processing and Space Physics. She has been evincing keen interest in scientific writing in creating public awareness. Dr Kavitha authored half a dozen books aimed at students, scholars and scientific community.

Mr. Ramesh Gorrepotu is pursuing his doctoral degree at the Department of Physics and Electronics, Institute of Science, GITAM (deemed to be University) in the field of Embedded Systems. He is an experienced Telecommunication and IP Networking engineer.

Mr. Korivi Narendra Swaroop is pursuing his doctoral degree at the Department of Physics and Electronics, Institute of Science, GITAM (deemed to be University) in the field of Embedded Systems. He has Overall 14+ Years of experience in Independent Verification and validation of Embedded and Application Software System's

Dr. Madhavaprasad Dasari Associate Professor in the Department of Electronics and Physics in GITAM (deemed to be) University, Visakhapatnam. He received M.Sc. from Acharya Nagarjuna University, Guntur and Ph.D. from Andhra University, Visakhapatnam. His research interests include ceramics, ceramic composites, nano materials for the applications of dielectric, ferroelectrics, piezoelectrics and DMS with different processing and characterization methods. He has authored/co-authored over 40 research articles in various national and international journals. He has currently taken up a research project funded by UGC-DAE-CSR.